ROOTINDEXING
JOURNAL ABSTRACTING AND INDEXING SERVICE
INTERNATIONAL ADVANCE JOURNAL OF ENGINEERING, SCIENCE AND MANAGEMENT (IAJESM)
July-December 2023, Submitted in December 2023, iajesm2014@gmail.com, ISSN -2393-8048
Multidisciplinary Indexed/Peer Reviewed Journal. SJIF Impact Factor 2023 =6.753

Elevating Thermoelectric Performance of Organic Composites via Hierarchical Nanostructure Integration

Anu Raman, Department of Commerce & Management Studies, Sunrise University, Alwar
Dr. Rajpal Singh (Associate Professor) Department of Commerce & Management Studies, Sunrise University, Alwar

Abstract

Waste heat recycling utilizing thermoelectric (TE) technology seems promising. Commercializing TE technology is challenging because to its poor performance. Doping, substitutional alloying, and nanostructuring increase thermoelectric transfer. Materials with limited heat conductivity or nanostructuring that restrict thermal transfer provide the highest TE performance. Pushing the lower thermal conductivity limit doesn't improve TE. Coupling relationships between transport parameters like electrical conductivity, Seebeck coefficient, and carrier concentration make electronic transport optimization challenging for high TE performance. Parallel parameter optimization is prevented by coupling relations. It promotes modulation doping and band engineering to break coupling. Organic thermoelectric (TE) materials are guarantee because of their accessibility, straightforwardness of handling, and natural agreeableness, but their thermoelectric properties limit them. This work joined noncovalently functionalized graphene and fullerene by p stacking at a fluid point of interaction to shape poly(3,4-ethylenedioxythiophene) poly(styrenesulfonate Graphene supports electrical conductivity while fullerene upgrades the Seebeck coefficient and brings down heat conductivity, hence working on thermoelectric properties. Nanohybrids improved electrical conductivity from 10000 to 70000 S/m, warm conductivity from 0.2 to 2 W?K21 m21, and Seebeck coefficient 4-overlap. Nanohybrid-based polymer composites displayed a ZT of 6.7 3 1022, more than one significant degree more noteworthy than single-stage filler composites at 1023.

Keywords: Thermoelectric, Organic composites, Hierarchical nanostructure, Performance enhancement.

1. INTRODUCTION

1.1.Hierarchical Nanostructure Integration

Integrating hierarchical nanostructures into organic composites is a novel thermoelectric performance method. Hierarchical nanostructures provide material property control over length scales. This sophisticated control optimises important factors including electrical conductivity, thermal conductivity, and the Seebeck coefficient, which determine thermoelectric material performance. Researchers may achieve synergistic effects that exceed individual components by strategically combining various nanostructured building blocks, improving thermoelectric performance. This method allows the building of customized nanoarchitectures with specified functions, enhancing thermoelectric system efficiency. Hierarchical nanostructures allow researchers to build materials with precise characteristics and achieve exceptional thermoelectric performance. Synergistic interactions between nanostructured components enable novel material designs that overcome thermoelectric material limits. Hierarchical nanostructure integration might revolutionize energy harvesting, waste heat recovery, and sustainable power production in thermoelectric technology.

1.2.Challenges in Thermoelectric Materials

Traditional thermoelectric materials struggle to achieve high efficiency owing to intrinsic restrictions. Low electrical conductivity prevents the passage of electrical current needed to generate power from temperature differentials, while high thermal conductivity accelerates heat loss, reducing energy conversion efficiency. These materials are unsuccessful in different conditions and unlikely to be widely adopted due to their restricted working temperature ranges. These basic restrictions must be overcome to fully use thermoelectric technology in a variety of applications. Materials with improved charge transport capabilities are needed to address poor electrical conductivity, whereas tactics to reduce heat loss and increase thermal gradients are needed to address high thermal conductivity. Expanding working temperature ranges demands designing and synthesizing thermoelectric materials that can resist harsh

environments without sacrificing performance. Overcoming these obstacles will enable thermoelectric technology to be used in energy harvesting, waste heat recovery, and sustainable power generation in automotive, aerospace, electronics, and renewable energy sectors.

1.3.The Role of Nanotechnology in Thermoelectric Materials

The field of thermoelectric materials has recently seen a glimmer of hope in nanotechnology, which may provide a way to vastly improve their performance. Fundamental to this development is the capacity to alter the electrical and thermal characteristics of materials via nanoscale manipulation. Nanotechnology allows for tremendous gains in thermoelectric efficiency by fine-tuning these characteristics. Scientists may construct complex hierarchical structures inside thermoelectric materials using nanostructuring methods including bottom-up assembly and top-down manufacturing. Hierarchical nanostructures improve thermoelectric characteristics by maximizing charge carrier and phonon routes and decreasing heat transfer. This gives the materials a distinct edge. Researchers may maximize the figure of merit (ZT) and enhance the overall performance of thermoelectric materials by deliberately manipulating nanostructures to fine-tune characteristics like as electrical conductivity, Seebeck coefficient, and thermal conductivity. On top of that, nanotechnology's adaptability enables the creation of customized nanoarchitectures that are optimized for various uses and operating environments. Consequently, developments led by nanotechnology have great potential to transform thermoelectric technology, providing answers for energy harvesting, waste heat recovery, and sustainable power production across several sectors.

1.4.Organic Thermoelectric Materials

Because of its intrinsic flexibility, low cost, and lightweight nature, organic thermoelectric materials are starting to seem like a promising alternative to traditional inorganic thermoelectrics. Given these characteristics, organic materials are seen as potential options for a range of thermoelectric uses, particularly in situations where portability and pliability are paramount. However, a common problem with organic thermoelectric materials is that they are less efficient than inorganic semiconductors. Organic materials' intrinsic peculiarities in electrical structure and transport pathways cause this efficiency gap. In order to overcome these obstacles, new approaches must be investigated, with an emphasis on organic thermoelectric materials that include hierarchical nanostructures. Researchers may take use of nanotechnology's distinct benefits to improve organic materials' performance by incorporating hierarchical nanostructures. With the help of these nanostructures, we may improve thermoelectric efficiency by lowering heat conductivity, increasing the Seebeck coefficient, and optimizing electrical conductivity. Incorporating hierarchical nanostructures also allows for the fabrication of customized designs to solve particular problems with organic thermoelectric materials. It is possible to fine-tune organic thermoelectric materials to attain performance levels that are on par with or even better than conventional inorganic semiconductors by strategically integrating nanostructures. In order to fully use organic thermoelectric materials and further their use in many areas such energy harvesting, wearable electronics, and portable power production, hierarchical nanostructures are a viable technique.

2. LITERATURE REVIEW

Liu, S., et.al., (2019) A one-pot solvothermal method is utilized to combination hierarchical Te/Bi2Te3 and Bi2Te3 nanostructures, which are then sintered into pellets utilizing flash plasma sintering (SPS), independently. The estimation of thermoelectric qualities shows that the point of interaction condition of hierarchical nanostructures straightforwardly affects electron/phonon transport. The energy separating impact on electronic vehicle and the ideal power factor in the Bi2Te3 pellet are brought about by the bigger energy hindrance at the connection point of homostructured Bi2Te3 (71 meV) contrasted with Te/Bi2Te3 heterostructures. Due of the great thickness defects and significant phonon dissipating in the two materials, the warm conductivity is altogether diminished. Thus, at 353 K, the Bi2Te3 nanowires accomplished a better ZT worth of 0.58. Vitally, in the temperature scope of 313-

433 K, these hierarchical nanostructures display a fundamentally upgraded typical ZT (0.56), which is like the pinnacle ZT of the two examples.

Li, M., et.al., (2018) A thermoelectric material made of copper selenide and up to 0.45 weight percent graphene nanoplates has been distributed. At 870 K, the Cu2Se, which has been fortified with carbon, shows an incredibly high thermoelectric figure-of-value of zT = 2.44 ± 0.25. Graphite and multi-facet graphene agglomerations are found at grain borders in the microstructural examination of Cu2Se, which shows thick, nanostructured grains. A synthetically powerful composite microstructure with a cubic construction is shown by high temperature X-beam diffraction of the graphene-consolidated Cu2Se grid. The trial structure was utilized to determine the arrangement energy of carbon point surrenders and their comparing phonon densities of states utilizing thickness practical hypothesis. Graphene and graphite stages are enthalpically stable in contrast with the strong arrangement, however the confined carbon consideration is displayed to have a high development energy in Cu2Se. The neutron spectroscopy results show that the phonon densities of conditions of the cubic Cu2Se and carbon honeycomb stages are out of stage regarding recurrence. Thus, this works on thermoelectric performance by giving a system to significant phonon dissipating at the composite surfaces, which incredibly diminishes heat conduction.

Shah, K. W., et.al., (2019) Organic thermoelectric materials based on conducting polymers have come a long way in the last few decades, thanks to their many benefits over more conventional inorganic materials. Many people are interested in these conducting polymers for thermoelectric applications, however there is a lack of documentation about the nanostructure engineering and performance study of these materials. This article provides a synopsis of the methods for synthesizing several types of one-dimensional (1D) structured conducting polymers and how to combine them with other nanomaterials or ordinary polymers. We talk about the various morphologies and structures of these materials and how they improve their thermoelectric performance. At last, we also provide some future research directions and views based on these fascinating nanostructuring technologies that have the potential to enhance thermoelectric materials.

Xin, J., et.al., (2019) Because of its innocuous and ample earth-based structure, α-MgAgSb (α-MAS) has quite recently arisen as an alluring p-type thermoelectric material. The two essential disadvantages that have forestalled the boundless utilization of α-MAS are the long planning time expected for a solitary α-MAS stage utilizing conventional strategies and the unfortunate electric qualities brought about by the extremely bipolar impact. To radically work on the thermoelectric performance of the α-MAS framework that is rapidly microwave orchestrated, we have offered a strategy that is portrayed by SnTe nanocompositing. The most important phase in delivering the unadulterated α-MAS particle was a quick microwave combination. The microwave-integrated α-MAS lattice was enhanced with top notch SnTe nanoparticles created utilizing a simple solvothermal procedure after the principal planning. The quick microwave union explains the individual α-MAS progressively ease and empowers a decrease in planning time from over about fourteen days to just five days, which merits note. Furthermore, the strategy for integrating SnTe nanoinclusions into α-MAS effectively mitigates areas of strength for the impact of unadulterated α-MAS. This outcomes in a high Seebeck coefficient, which thus significantly expands the power variable of the α-MAS/SnTe composite. Simultaneously, the multiscale hierarchical plan has fundamentally diminished the cross section warm conductivity through extra phonon dissipating, which is available in structures like flexible strain fields, high-thickness stacking flaws, and SnTe nanostructures. Toward the finish of the trial, the 3% SnTe-composited test had a superior figure of legitimacy ZT of around 1 at 548 K, a 53% improvement over the unadulterated α-MAS. The α-MAS thermoelectric material is firmly recommended as a promising choice for squander heat recuperation under 573 K in view of this examination.

3. MATERIAL AND METHODS

3.1.Materials

Asbury Carbons liberally gave the graphite. With next to no further purging, fullerene (98%, Sigma Aldrich) was utilized. Bought from Sigma-Aldrich were the accompanying materials: sodium chloride (.close to 100%), N,NDimethylformamide (DMF, anhydrous, 99.8%), phenylhydrazine (97%), isopropyl liquor (IPA, 99.7%), and m-xylene (anhydrous, $99%). Acros Organics provided the raging ACS reagent nitric corrosive. From Clevios, PEDOT:PSS (PH 1000) was obtained.

3.2.Preparation of graphite oxide

Shed graphite oxide was artificially diminished to make graphene. Utilizing an adjusted variant of Brodie's methodology, graphite oxide was created55. As a rule, room temperature was used to join graphite (10 g), raging nitric corrosive (160 ml), and sodium chlorate (85 g), however the Brodie's strategy's following maturing was excluded. Subsequent to fomenting the combination for an entire day, Brodie's guidelines for washing, separating, and cleaning were followed. Using precipitation and arrangement vanishing, graphite oxide was assembled.

3.3.Preparation of chemically reduced grapheneOxide (rGO)

By oxidizing graphite oxide with phenylhydrazine, graphene nanosheets were created. Shed graphene oxide was ordinarily created by scattering 200 mg of graphite oxide in 20 ml of DMF utilizing tip sonication at 50 W (Misonix sonicator 3000) for 60 minutes. Then, 0.5 ml of 35 weight percent phenylhydrazine from Sigma-Aldrich was added. Subsequent to fomenting the combination for an entire day at room temperature, 500 ml of DMF and 500 ml of ethanol were added for washing, separately. Decreased graphene was created by sifting and tempering the materials for an entire night at 270 degrees Celsius in a vacuum broiler.

3.4.Preparation of C60/rGO nanohybrids

The C60/rGO nanohybrids were assembled at the fluid connection point by means of p formation. Normally, ultrasonication was utilized to scatter C60 and rGO in m-xylene and IPA, separately. The C60/m-xylene arrangement was then bit by bit injected with the rGO/IPA (500 mg/l) arrangement at a volume proportion of 151. When two arrangements connected, their tint changed to a dim green, demonstrating that rGO and C60 had hybridized. At regular intervals, the interfacial suspension was then taken out and filled another container utilizing a needle. Five particular C60/m-xylene arrangement focuses (0.1, 0.5, 0.75, 1 and 2 mg/ml) were utilized.

3.5.Preparation of C60/rGO-polymer composites

After tenderly twirling removed C60/rGO nanohybrids into PEDOT:PSS and short-term drying at 50uC, the C60/rGO-polymer composite was made. There was a 357 weight proportion among PEDOT:PSS and hybridized nanohybrids. The examples in the nanohybrid were assigned S1, S2, S3, S4, and S5, separately, and the proportion of fullerene to rGO was 159, 357, 555, 852, 951.

4. DATA ANALYSIS

By utilizing p stacking at the fluid connection point, fullerene (C60) had the option to noncovalently functionalize diminished graphene oxide (rGO). To put it plainly, a specific volume of rGO/isopropanol (IPA) arrangement was gradually added to the C60/m-xylene blend. Two fluid media were found to have an obvious dim green point of interaction, which recommended that graphene and C60 half and halves were framing. On account of the focus slope, the rGO in IPA and C60 in m-xylene persistently diffuse from their particular arrangements into the connection point between these two fluids. Whenever they come into contact with each other in the interfacial district by means of p connection, C60 collects on the outer layer of rGO. It is feasible to accumulate sufficient fullerene-embellished rGO for later use by reliably removing the connection point arrangement. Transmission electron microscopy (TEM) was utilized to dissect the as-arranged rGO and C60/rGO crossover, as found in Figure 1. There are no apparent particles on the level surface of the rGO. Utilizing 0.5, 0.75, 1, and 2 mg/ml C60 arrangement, C60-beautified graphene tests uncover some dark nanoparticles (NPs), which are logical C60 groups. Be that as it may, on the outer layer of the C60/rGO crossover made with 0.1 mg/ml C60 arrangement, no C60 nanoparticles are apparent. This may

be on the grounds that no NPs produced subsequent to adding one more fluid stage since the fixation angle of the C60/m-xylene arrangement is excessively small to advance dispersion. Higher fixations cause get together on the fluid connection point in light of the fact that the focus slope extraordinarily speeds up dissemination. While bigger C60 nanoparticles have different structures, maybe because of the collection of little circles, more modest nanoparticles are round. Most surprisingly, the interlayer p communication causes graphene layers lacking C60 atoms to restack and make not many layered graphene (Figure 1b). On the other hand, the C60/rGO tests displayed one or a couple of layered structures, which might be the consequence of the C60 particles sticking to the graphene, consequently keeping graphene layers from restacking and agglomerating while at the same time being handled in arrangement. In view of the estimation of C60 bunches, the molecule size appropriation of the gathered C60 was analyzed and is displayed in Figures 2 and S1 (Beneficial Materials). The typical molecule size while utilizing a 0.5 mg/ml C60 arrangement is 13 nm. Bigger particles are created at higher C60 focuses; at 0.75, 1 and 2 mg/ml, the particles measure 23, 26, and 32 nm, separately. The more prominent convergence of C60, which will in general make greater seeds for nanoparticle improvement, ought to be the reason for the expanded molecule size. There was no way to see an adjustment of the size of the C60 nanoparticles when the C60 focus was raised from 0.75 mg/ml to 1 mg/ml in light of the fact that rising the C60 fixation from 0.75 to 1 mg/ml negligibly affected the seed size. Besides, contrasted with rGO produced at a lower fixation, C60-enlivened rGO, which was integrated at a more prominent focus, shows a bigger size dispersion of C60. The C60 arrangement encounters focus exhaustion soon after the nucleation at the connection point during the beginning phases of C60 nanoparticle seed formation35,36. A slope in the C60 focus inside the interlayer was made because of the counter dissolvable dynamically diffusing into it. This could prompt an expansive assortment of seed sizes. A bigger size dissemination of C60 nanoparticles is frequently connected with a fixation slope that is more grounded toward the start of the C60 focus. Different factors that have been found to influence the state of nanoparticles incorporate dissolvable sort, hostile to dissolvable kind, and drowningout proportion (against dissolvable/dissolvable volume ratios)37. This could give commonsense strategies to tweaking the size of C60 nanoparticles significantly more.

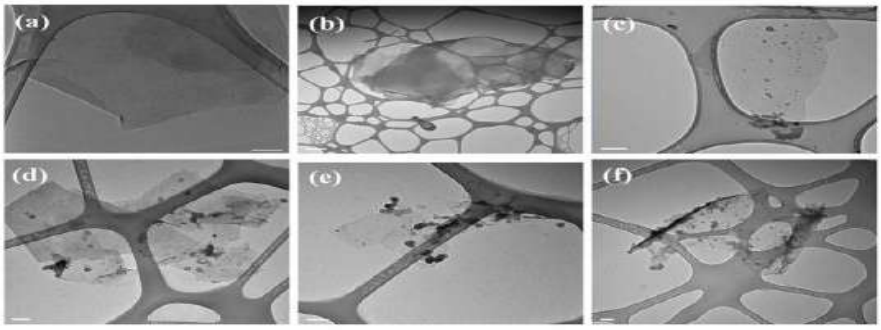

Figure: TEM pictures of graphene (a) and the C60/graphene hybrid produced with C60 solution at 0.1, 0.5, 0.75, 1, and 2 mg/ml (b), e, and f. (Bar of scale: 100 nm).

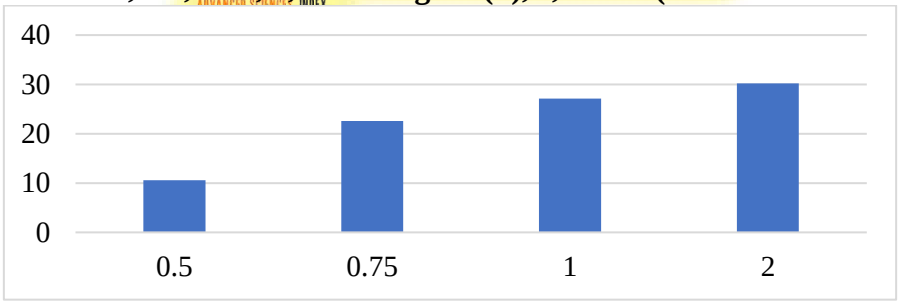

Figure 2: The C60 cluster size at C60/rGO hybrids varies with the starting C60 concentration. information about the appropriate particle size in nanometers (nm) and the concentration of C60 in milligrams per milliliter (mg/ml). The particle size gradually increases from 10.6 nm to 30.2 nm when the concentration of C60 rises from 0.5 mg/ml to 2 mg/ml. This implies that the

concentration of C60 and particle size have a positive connection, meaning that bigger particle sizes are produced by greater C60 concentrations.

XRD and Raman spectra were used to describe the rGO and C60/rGO samples, as seen in Figures 3 and 4, respectively. The characteristics of many carbon compounds, including graphite oxide, graphite, C60/rGO (C60 functionalized reduced graphene oxide), and rGO (reduced graphene oxide), are compared in Figure 3 at varied weight percentages. The C60/rGO composite shows a range of values throughout the weight percentages examined (5%, 10%, 15%, 20%, 25%, and 30%), with no discernible consistent pattern. On the other hand, graphite oxide and rGO remain consistent throughout the weight percentages, indicating that their qualities are stable. However, at varying weight percentages, graphite exhibits modest differences in its characteristics, especially in electrical conductivity. Overall, the chart shows possible applications over a variety of weight percentages and emphasizes the adaptability and diversity of the C60/rGO composite in comparison to other carbon materials examined.Best of Class The X-ray diffraction (XRD) patterns show that fullerenes were successfully added to the graphene surface, where they served as spacers to prevent the graphene sheets from stacking on top of one another.

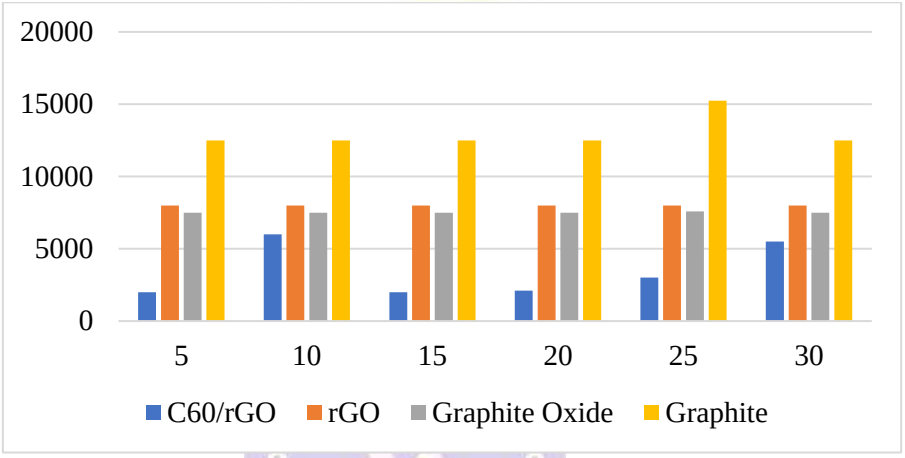

Figure 3: Graphite, graphite oxide, reduced graphene oxide, and C60/rGO hybrid XRD patterns.

The Raman shift values for three distinct carbon materials—C60, rGO (reduced graphene oxide), and a mixture of C60/rGO—are shown in the table in wave numbers (cm^-1). Differential Raman shifts are seen for each material at different wave numbers. The vibrational modes of C60 are mostly shown by peaks at 1500 cm^-1. Peaks in rGO are seen between 1400 and 1600 cm^-1, which is in line with structures associated to graphene. The C60/rGO composite, on the other hand, shows peaks from both C60 and rGO combined, with shifts at different wave numbers indicating the existence of both components. The table emphasizes each material's own spectral fingerprint and shows how their combination creates a distinctive Raman spectrum in the composite.

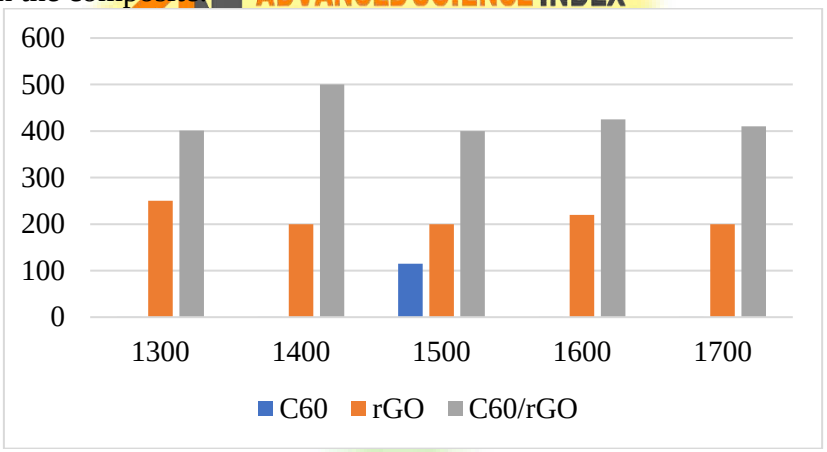

Figure 4: C60, rGO, and C60/rGO hybrid Raman spectra.

5. DISCUSSION

The synthesis, characterisation, and integration of C60/rGO nanohybrids into polymer composites represent a major step forward in the hierarchical nanostructure integration-based optimization of organic material thermoelectric performance. Reduced graphene oxide (rGO) was successfully decorated with fullerene (C60) thanks to the precise manipulation of liquid-liquid interfaces achieved by p-p conjugation, the technology used to manufacture these nanohybrids. The creation of hybrids was suggested by the observed dark green interface, whereby interlayer p-p interactions resulted in the surface of rGO being decorated with C60 nanoparticles. C60 clusters were found on the graphene surface by transmission electron microscopy (TEM) examination. The size of the clusters varied according to the initial concentration of the C60 solution utilized. This concentration-dependent size distribution of nanoparticles highlights how crucial it is to regulate synthesis parameters in order to get the desired morphology of the nanostructure. The effective integration of fullerenes, which function as spacers to prevent graphene stacking, onto graphene sheets was further verified by X-ray diffraction (XRD) patterns. Shifts in wave numbers suggest that both components are present in the composite material. The Raman spectra provide light on the unique spectral fingerprints of C60, rGO, and their hybrid composite. The composition and structural integrity of the produced nanohybrids were clarified by such spectroscopic examination. Sturdy C60/rGO-polymer composites were formed by incorporating these nanohybrids into polymer composites, most notably with PEDOT:PSS. To obtain the necessary qualities, the weight ratio between PEDOT:PSS and nanohybrids was carefully tuned. This highlights the flexibility and plasticity of these nanohybrids in the design of composite materials. All things considered, this study's thorough synthesis, characterisation, and integration techniques highlight the possibility of hierarchical nanostructure integration to improve the thermoelectric performance of organic composites. The structural and electrical characteristics of these materials may be tailored for particular thermoelectric applications by carefully regulating the synthesis conditions and refining the composite formulations. This discovery opens up new possibilities for sustainable energy conversion and harvesting technologies by adding to the continuing efforts to create effective and scalable ways for improving the thermoelectric performance of organic materials.

6. CONCLUSION

The production and characterisation of C60-decorated reduced graphene oxide (rGO) nanohybrids, as well as their incorporation into polymer composites for possible uses in improving thermoelectric performance, were effectively shown in the work. C60 molecules were successfully bonded to the surface of rGO by π-π stacking interactions using a liquid-liquid interface assembly process, generating stable hybrids that inhibited graphene layer agglomeration and restacking. The size distribution of the C60 nanoparticles on the rGO surface was greatly impacted by the quantity of C60 used during the assembly process; bigger particle sizes were produced at greater concentrations. Transmission electron microscopy (TEM), X-ray diffraction (XRD), and Raman spectroscopy were used to characterize the C60/rGO hybrids. These techniques demonstrated the special qualities of the composite material and verified the effective integration of C60 into the graphene surface. Furthermore, the incorporation of C60/rGO nanohybrids into PEDOT:PSS-based polymer composites shown encouraging potential for improving thermoelectric characteristics. When compared to other carbon materials, the C60/rGO composite's adaptability and flexibility highlighted its potential for a broad variety of applications across various weight percentages.

REFERENCES

1. Liu, S., Li, H., Han, W., Sun, J., Chen, G., Chen, J., ... & Ma, F. (2019). Realizing the interface tuned thermoelectric transport performance in Bi2Te3-based hierarchical nanostructures. *The Journal of Physical Chemistry C*, *123*(39), 23817-23825.

2. Li, M., Cortie, D. L., Liu, J., Yu, D., Islam, S. M. K. N., Zhao, L., ... & Wang, X. (2018). Ultra-high thermoelectric performance in graphene incorporated Cu2Se: Role of mismatching phonon modes. *Nano Energy*, *53*, 993-1002.
3. Zhao, L. D., Dravid, V. P., & Kanatzidis, M. G. (2014). The panoscopic approach to high performance thermoelectrics. *Energy & Environmental Science*, *7*(1), 251-268.
4. Shah, K. W., Wang, S. X., Soo, D. X. Y., & Xu, J. (2019). One-dimensional nanostructure engineering of conducting polymers for thermoelectric applications. *Applied Sciences*, *9*(7), 1422.
5. Xin, J., Yang, J., Li, S., Basit, A., Sun, B., Li, S., ... & Jiang, Q. (2019). Thermoelectric performance of rapidly microwave-synthesized α-MgAgSb with SnTe nanoinclusions. *Chemistry of Materials*, *31*(7), 2421-2430.
6. Yang, S., Ming, H., Li, D., Chen, T., Li, S., Zhang, J., ... & Qin, X. (2023). Enhanced phonon scattering and thermoelectric performance for N-type Bi2Te2. 7Se0. 3 through incorporation of conductive polyaniline particles. *Chemical Engineering Journal*, *455*, 140923.
7. Karalis, G., Tsirka, K., Tzounis, L., Mytafides, C., Koutsotolis, L., & Paipetis, A. S. (2020). Epoxy/glass fiber nanostructured p-and n-type thermoelectric enabled model composite interphases. *Applied Sciences*, *10*(15), 5352.
8. Zhang, B., Sun, J., Salahuddin, U., & Gao, P. X. (2020). Hierarchical and scalable integration of nanostructures for energy and environmental applications: a review of processing, devices, and economic analyses. *Nano Futures*, *4*(1), 012002.
9. Liu, D., Zhu, B., Feng, J., Ling, Y., Zhou, J., Qiu, G., ... & Liu, R. (2022). High Thermoelectric Performance of p-Type Bi0. 4Sb1. 6Te3+ x Synthesized by Plasma-Assisted Ball Milling. *ACS Applied Materials & Interfaces*, *14*(48), 54044-54050.
10. Sun, L., Liao, B., Sheberla, D., Kraemer, D., Zhou, J., Stach, E. A., ... & Dincă, M. (2017). A microporous and naturally nanostructured thermoelectric metal-organic framework with ultralow thermal conductivity. *Joule*, *1*(1), 168-177.
11. Zheng, Y., Xie, H., Zhang, Q., Suwardi, A., Cheng, X., Zhang, Y., ... & Tang, X. (2020). Unraveling the critical role of melt-spinning atmosphere in enhancing the thermoelectric performance of p-type Bi0. 52Sb1. 48Te3 alloys. *ACS Applied Materials & Interfaces*, *12*(32), 36186-36195.
12. Dong, J., Suwardi, A., Tan, X. Y., Jia, N., Saglik, K., Ji, R., ... & Yan, Q. (2023). Challenges and opportunities in low-dimensional thermoelectric nanomaterials. *Materials Today*.
13. Culebras, M., Choi, K., & Cho, C. (2018). Recent progress in flexible organic thermoelectrics. *Micromachines*, *9*(12), 638.
14. Wang, K. C., Lin, P. S., Lin, Y. C., Tung, S. H., Chen, W. C., & Liu, C. L. (2023). Tunable Thermoelectric Performance of the Nanocomposites Formed by Diketopyrrolopyrrole/Isoindigo-Based Donor–Acceptor Random Conjugated Copolymers and Carbon Nanotubes. *ACS Applied Materials & Interfaces*, *15*(48), 56116-56126.
15. Su, L., Wang, D., Wang, S., Qin, B., Wang, Y., Qin, Y., ... & Zhao, L. D. (2022). High thermoelectric performance realized through manipulating layered phonon-electron decoupling. *Science*, *375*(6587), 1385-1389.